Nanostructured ZnO and CuI Thin Films on Poly(Ethylene Terephthalate) Tapes for UV-Shielding Applications

N.P. Klochko[1], K.S. Klepikova[1,*], D.O. Zhadan[1], V.R. Kopach[1], I.V. Khrypunova[1], S.I. Petrushenko[2], S.V. Dukarov[2], V.M. Lyubov[1], A.L. Khrypunova[1]

[1] *National Technical University "Kharkiv Polytechnic Institute", 2, Kyrpychova St., 61002 Kharkiv, Ukraine*
[2] *V.N. Karazin Kharkiv National University, 4, Svobody Square, 61022 Kharkiv, Ukraine*

In this work, we study a suitability for protection against terrestrial ultraviolet part of the solar spectrum of undoped and doped by indium zinc oxide thin nanostructured films, ZnO and ZnO:In, respectively, and cuprous iodide (CuI) films obtained via Successive Ionic Layer Adsorption and Reaction (SILAR) techniques on the lightweight low cost poly(ethylene terephthalate) (PET) flexible substrates. The film morphology is observed by scanning electron microscopy (SEM). Chemical compositions of the films are investigated by X-ray fluorescence (XRF) microanalysis. To research crystal structure we used X-ray diffraction (XRD) method. The UV-protection ability of the nanostructured thin films, PET tapes and samples consisting of the PET substrates and the films deposited on them by the SILAR method has been evaluated on the base of their optical properties in accordance with an international standard ISO 2443:2012(E) "Determination of sunscreen UVA photoprotection in vitro". According to the research, nanostructured ZnO, ZnO:In and CuI thin films made by the cheap, affordable, and suitable for mass production SILAR method on thin flexible cheap PET substrates have been proposed as a new material for UV-shielding applications. In accordance with an international standard ISO 2443:2012(E), UV-protection ability of the samples consisting of the PET substrates and the films deposited on them by the SILAR method fits the category "excellent" (50+). The best low cost flexible and lightweight UV shielding material turned out to be that consisted from ZnO:In film and PET substrate, the sun protection factor of which equals 157.

Keywords: ZnO, CuI, Poly(ethylene terephthalate), Ultraviolet radiation, Sun protection factor.

1. INTRODUCTION

According to [1-6], since ultraviolet (UV) radiation triggers the formation of free radicals, the long-term exposure of human skin to UV radiation can result in health issues, such as aging, DNA damage, skin reddening, acne, and even skin cancer. UV light also has degradation effects on various materials, such as polymers, dyes, pigments and semiconductor devices [6]. Therefore, interest in the creation of light and flexible shields with variable shapes, which are capable of providing protection from solar UV, is particularly due to the need to reduce the risk of skin cancer and to prevent skin injury associated with UV exposure [1-9]. Extensive research efforts were focused on the development of UV shielding material, which may be efficient for UV protective coating [1-9], especially in the wavelength (λ) range 290-400 nm (terrestrial UV part of the solar spectrum, namely 95 % UVA (320-400 nm range) and 5 % UVB (290-320 nm range)). Generally, modern materials for sun protection contain nanoparticles or nanostructured layers of wide band gap semiconductors (mainly titanium dioxide (TiO_2) or zinc oxide (ZnO)), whose large surface area-to-volume ratio significantly increases the effectiveness to block UV radiation when compared to bulk materials [1-7]. Among them, the best choices for UV protection are nanostructured thin ZnO films [1, 4] or indium doped ZnO:In films [1], hierarchical ZnO nanostructures [8], ZnO quantum dots [9], ZnO-polystyrene nanocomposite films [6], ZnO quantum dots/sodium carboxymethyl-

cellulose nanocomposite polymer films [2], and fibrous ZnO/polyvinyl alcohol composite membranes [5]. At the same time, we were not able to find in the literature examples of the use of a wide-gap semiconductor cuprous iodide (CuI) as the UV-shielding material. However, it is indicated in [10-12] that CuI thin films and the solutions contained nanosized CuI particles demonstrated a strong absorbance of the UVA light. By the way, cuprous iodide similarly to zinc oxide exhibits photocatalytic properties with respect to organic contaminants [12] and it has a potential implication in antibiotic therapy as an antibacterial agent [13]. Therefore, in this work, we carry out a comparative analysis of the UV-shielding properties of the nanostructured ZnO, ZnO:In and CuI thin films.

As UV protective canopies and other UV shields should have large areas, a preference must be given to affordable and mass-production deposition methods. Among such methods, Successive Ionic Layer Adsorption and Reaction (SILAR) technique allows deposition of the nanostructured doped and undoped ZnO [14] and CuI [11, 15] thin films over large areas and suggests low capital expenditure based on simple process equipment.

The aim of the present work is to study suitability for protection against UV radiation of undoped and doped with indium zinc oxide thin films, ZnO and ZnO:In, respectively, and CuI films obtained via different SILAR techniques on the poly(ethylene terephthalate) (($C_{10}H_8O_4$)$_n$ or PET) flexible substrates, which were chosen due to the lightweight, low cost and availability. Here we investigate the crystal structure,

---

* catherinakle@gmail.com

chemical composition, optical properties and surface morphology of the manufactured ZnO, ZnO:In and CuI films. The UV-protection ability of the nanostructured ZnO, ZnO:In and CuI thin films, PET tapes and samples consisting of the PET substrates and films deposited on them by the SILAR method has been evaluated in accordance with an international standard ISO 2443:2012 (E) "Determination of sunscreen UVA photoprotection in vitro".

2. EXPERIMENTAL DETAILS

In this study, ZnO, ZnO:In and CuI thin films were synthesized via different SILAR techniques on the flexible and transparent 20 μm thick and 3 cm wide PET tapes (Toray Industries, Inc.).

The deposition techniques by means of SILAR of ZnO and ZnO:In films using the zinc sulfate cationic precursor were given by us earlier in [14]. In few words, we used from 20 to 400 deposition cycles of SILAR, which were carried out in an aqueous solution of $ZnSO_4$ and NH_4OH as cationic precursor. For the deposition of ZnO:In film via SILAR, the cationic precursor contained 2.7 M potassium hydroxide, 180 mM zinc oxide and additionally 9 mM $InCl_3$. In the SILAR process, one growth cycle included following three steps: (1) immersing of the substrate into cationic precursor for 10 s; (2) its immersing into anionic precursor, namely into hot (90 °C) water for 10 s; (3) rinsing of a flexible substrate in a separate H_2O beaker at room temperature for 5 s to remove loosely bound particles. The thickness of the obtained ZnO and ZnO:In films on PET substrates (t in the 0.1-3.8 μm range) was determined gravimetrically, taking for the t calculation the bulk ZnO density of 5.61 g/cm^3. As seen from Table 1, three SILAR modes differ from each other by the film thickness through an adjusting the number of SILAR cycles, by the presence or absence of In in the films, and by the application or not of the initial step for a creation of a bonding seed layer to ensure an adhesion of zinc oxide film with PET. The bonding seed layer was deposited by means of 10 or 20 times repeating process of dipping the PET substrate into aqueous solution contained ZnO and NH_4OH for 30 s and drying with hot air as described in [14].

Deposition of copper iodide films via SILAR was carried out at room temperature in accordance with [15] using an aqueous solution containing 0.1 M $CuSO_4$ and 0.1 M $Na_2S_2O_3$ as the cationic precursor, where a copper (I) thiosulfate complex $Na[Cu(S_2O_3)]$ was formed, from which Cu^+ ions were released into solution. The PET substrates were immersed into the cationic precursor for 20 s. Then, the substrates were washed in distilled water for 10 s. For the reaction of the strongly adsorbed Cu^+ ions on the PET surface with I^- ions to obtain some CuI monolayers, the substrate was then immersed for 20 s into aqueous NaI solution (anionic precursor), whose concentration was 0.05, 0.075 or 0.1 M. After that, the PET substrate with the thinnest CuI film was washed in distilled water for 10 s. The listed procedure was one SILAR cycle of CuI film deposition. Such SILAR cycles were repeated 40 times. As seen from Table 2, the thickness of the obtained CuI films was determined gravimetrically,

taking for the t calculation the bulk CuI density of 5.67 g/cm^3, t was in the 0.1-0.82 μm range.

Morphology of ZnO, ZnO:In and CuI thin films on PET substrates was observed by scanning electron microscopy (SEM) in a secondary electron mode as in [16]. For this, SEM instrument "Tescan Vega 3 LMH" operated at an accelerating voltage of 30 kV without the use of additional conductive coatings. To obtain SEM image of the uncoated dielectric PET substrate we used thin Cr film (~ 10-15 nm thick) as a conductive coating, which evaporated in vacuum at 10^{-6} Torr residual gas pressure immediately before its SEM research. Chemical analysis of the ZnO, ZnO:In and CuI films on PET was carried out by X-ray fluorescence (XRF) microanalysis using an energy dispersive spectrometry (EDS) system "Bruker XFlash 5010". Energy dispersion spectra were taken from the 50×50 μm of the uncoated PET substrate, ZnO, ZnO:In or CuI film areas. Quantification of the spectra was carried out in the self-calibrating detector mode.

To analyze the crystal structure of ZnO, ZnO:In and CuI films, we recorded X-ray diffraction (XRD) patterns by a "DRON-4" diffractometer. Scanning was performed with Bragg-Brentano focusing (theta – 2 theta). The presence of crystalline phases was revealed by comparing the experimental diffraction patterns with the reference database JCPDS by using PCPDFWIN v. 1.30 software. For the evaluation of the average crystallite size D we applied, in accordance with [11, 12], the X-ray line broadening method using the Scherrer's formula. Crystal lattice microstrains, which mainly were induced by the point defects, were obtained as $\varepsilon = \Delta d/d$ (where d is the crystal interplanar spacing according to JCPDS and Δd is the difference between the corresponding experimental and reference interplanar spacing). Dislocation density was evaluated through $1/D^2$ as in [14].

Optical properties of ZnO, ZnO:In and CuI thin films deposited via SILAR were studied with an "SF-2000" spectrophotometer equipped with "SFO-2000" specular and diffuse reflection attachment. Optical transmission spectra $T_0(\lambda)$ were recorded in the λ range 290-1100 nm, as control samples we used uncoated PET tapes. UV-absorption spectra we obtained in accordance with the international standard ISO 2443:2012 (E) "Determination of sunscreen UVA photoprotection in vitro" by means of calculation of absorbance $A(\lambda) = \lg(1/T_0(\lambda))$ in the 290-400 nm wavelength range. Spectra of diffuse reflectance $R(\lambda)$ were measured at light incidence angle $\vartheta = 8°$ relative to the normal to the surface. Optical band gaps for direct allowed transitions E_g of ZnO, ZnO:In and CuI films, which were translucent and characterized by large diffuse reflectance and negligible specular reflectance in the visible spectra, were determined as described in [12, 18] from the Kubelka-Munk function:

$$F(R) = \frac{(1-R)^2}{2R}. \tag{1}$$

As shown in [12, 18], the plots of $(F(R)\cdot h\nu)^2$ vs $h\nu$ yield the direct band gap values E_g of the materials by extrapolating $(F(R)\cdot h\nu)^2$ linear parts on $h\nu$.

UV-protection ability of ZnO, ZnO:In and CuI films deposited via SILAR on PET substrates was evaluated in accordance with an international standard ISO

2443:2012 (E) "Determination of sunscreen UVA photoprotection in vitro". For this, UV-absorption spectra $A(\lambda)$ were calculated from the experimental optical transmission spectra $T_0(\lambda)$ in the 290-400 nm λ range. Then, the sun protection factor (SPF, equivalent to an UV protection factor UPF) as a measure of the fraction of UV rays producing sunburn, which reach the skin, was calculated according to ISO 2443:2012 (E) as follows:

$$SPF = \frac{\int\limits_{\lambda=290}^{\lambda=400} E(\lambda) \cdot I(\lambda) \cdot d\lambda}{\int\limits_{\lambda=290}^{\lambda=400} E(\lambda) \cdot I(\lambda) \cdot 10^{-A_0(\lambda)C} \cdot d\lambda}, \qquad (2)$$

where $E(\lambda)$ is the erythemal action spectrum (data are given in Appendix C in the ISO 2443:2012(E)); $I(\lambda)$ is the spectral irradiance received from the UV source (solar simulated radiation) (data are given in Appendix C in the ISO 2443:2012(E)); $A_0(\lambda)$ is the mean monochromatic absorbance of the film before exposure to UV radiation; C is the coefficient of adjustment; $d\lambda$ is the wavelength step (1 nm).

As preliminary experiments showed [16], for our films $A_0(\lambda) \equiv A(\lambda)$, $C = 1$.

3. RESULTS AND DISCUSSION

Fig. 1 and Fig. 2 show typical SEM images and XRF data, correspondingly, for ZnO ($t = 3.8\,\mu m$) (a), ZnO ($t = 1.8\,\mu m$) (b) and ZnO:In ($t = 0.1\,\mu m$) (c) films deposited via different SILAR modes on PET. Chemical compositions of these ZnO and ZnO:In films obtained by the EDS microanalysis are presented in Table 1. Fig. 1d illustrates the SEM image of the uncoated PET tape. From the SEM images it is clear that undoped zinc oxide films are rather loose, therefore a large amount of carbon atoms, which are components of the PET tape composition $(C_{10}H_8O_4)_n$, are recorded in the XRF spectra in Fig. 2a and Fig. 2b, despite the ZnO thickness of 3.8 and 1.8 μm, respectively (compare EDS data in Table 1). At the same time, SEM image in Fig. 1c shows that ZnO:In film is quite dense, so its XRF spectral lines of zinc in Fig. 2c are greater than of carbon, notwithstanding the very small thickness of the ZnO:In film $t = 0.1\,\mu m$ (see EDS data in Table 1).

Analysis of XRD patterns of the same ZnO and ZnO:In films deposited via SILAR on PET substrates revealed (Fig. 3) that all films are single-phase and polycrystalline. The positions of the peaks in the XRD patterns in Fig. 3 consistent with polycrystalline wurtzite hexagonal ZnO structure (JCPDS #36-1451), including for the ZnO:In films, probably due to its low indium content (Table 1). The relatively high intensity of the ZnO reflections in the XRD pattern in Fig. 3a corresponds to the larger ZnO film thickness in comparison with the ZnO film in Fig. 3b. The indium doped zinc oxide film in Fig. 3c is textured in the <001> direction, as evidenced by the intensity of the (002) reflection in its XRD pattern. The halo from the semicrystalline PET substrate is especially clearly visible in the XRD pattern in Fig. 3c that is explained by the smallest ZnO:In film thickness ($t = 0.1\,\mu m$). Calculations of the grain sizes according to the Scherrer's method have shown (Table 1) that the average crystallite sizes D for
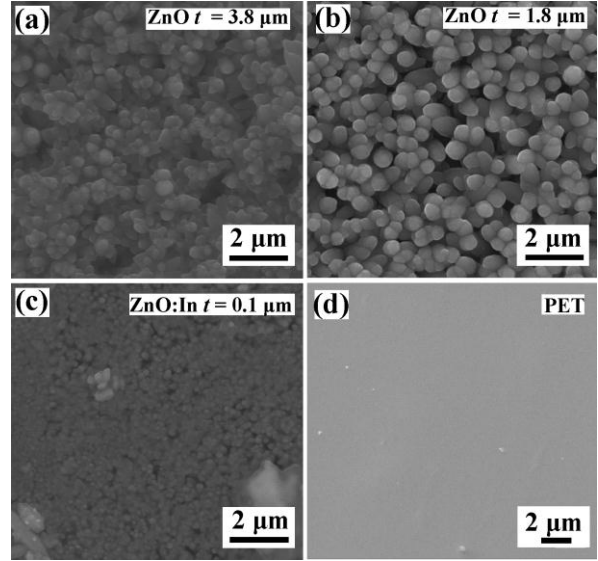

Fig. 1 – SEM images of ZnO (a, b) and ZnO:In (c) films with thickness t deposited via different SILAR modes on PET, and SEM image of the uncoated PET tape (d)
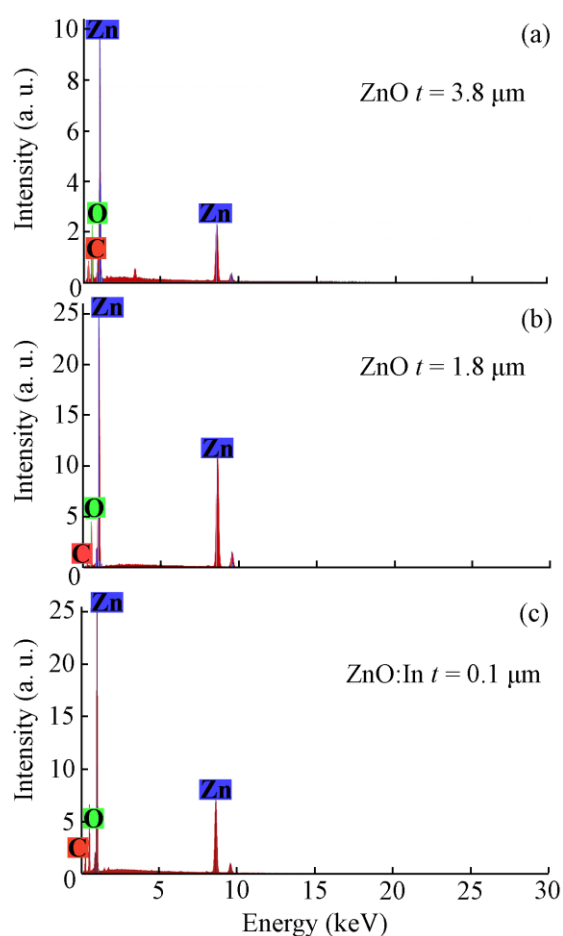
two ZnO films differ slightly and lie in the nanometer range, namely 20 nm for the thicker film and 17 nm for the thinner one. Their small dislocation densities $(2.5\text{-}3.5) \cdot 10^{15}$ lines/m² and low lattice microstrains $\varepsilon \approx (7\text{-}8) \cdot 10^{-3}$ a.u. are almost identical. According to the calculations presented in Table 1, the ZnO:In film has a slightly larger grain size $D \approx 25$ nm, lower dislocation density $1.6 \cdot 10^{15}$ lines/m² and lower lattice microstrains $\varepsilon \approx 5 \cdot 10^{-3}$ a.u.

Optical properties of these ZnO and ZnO:In films obtained in accordance with Table 1 on PET tapes via SILAR are presented in Fig. 4. It can be seen that 1.8 μm and 3.8 μm thick ZnO films are opaque in the visible range, their transparency T_0 does not exceed 1.5 %. Maximum transparency value of the thinnest ZnO:In film ($t = 0.1\,\mu m$) is greater, but T_0 does not exceed 35 % (Fig. 4a). The $T_0(\lambda)$ spectra in Fig. 4a do not contain interference extremes related to zinc oxide films, which is well explained by the surface morphology presented in Fig. 1a, b, c and is consistent with large diffuse reflectance in the entire visible range in Fig. 4b. As seen from Fig. 4c, the obtained band gap for direct optical transitions from the Kubelka-Munk function for the SILAR deposited ZnO and ZnO:In films is $E_g \approx 3.1$ eV. This value is close to the characteristic of zinc oxide $E_g = 3.37$ eV, although smaller, probably [19] due to the nanocrystalline structure of the films we made. From the absorption spectra in Fig. 4d, it is seen that the films doped with indium differ from those undoped by the increased B in the 290-308 nm range (part of the solar UVB). A similar feature was noted by the authors [1] who investigated the UV-protection ability of the nanostructured thin ZnO and ZnO:In films prepared via sol-gel deposition.

The ability of indium-doped film to absorb UVB more strongly is especially important, since solar light in the UVB range generally causes more serious damage than that in the UVA range. Due to its higher energy, UVB can cause acute sunburn and direct harm

Table 1 – SILAR modes for ZnO and ZnO:In films on PET substrates; thickness, chemical composition, crystal structure, and UV-shielding ability of these films

Material	Bonding seed layer	Number of SILAR cycles	Film thickness, μm	Chemical composition according to EDS, at. %				Crystal structure according to XRD			UV-protection factor SPF (290-400 nm)
				Zn	O	In	C	D, nm	$\varepsilon \cdot 10^3$, a.u.	$1/D^2 \cdot 10^{-15}$, lines·m^{-2}	
ZnO	–	400	3.8	9	50	–	41	20	7	2.5	35
ZnO	+ (10 times repeating)	100	1.8	11	44	–	45	17	8	3.5	37
ZnO:In	+ (20 times repeating)	20	0.1	33	50	< 1	17	25	5	1.6	116

Fig. 2 – XRF data of ZnO (a, b) and ZnO:In (c) films deposited via different SILAR modes on PET

to skin [3]; it leads to some forms of skin cancer, since the radiation directly damages DNA molecules in skin cells [6]. It can also be seen in Fig. 4d that the uncoated PET tape also absorbs ultraviolet in the 290-315 nm range, which is favorable for UV-shielding applications.

Sun protection factors calculated in accordance with an international standard ISO 2443:2012(E) for the deposited via SILAR on PET substrates ZnO and ZnO:In films are presented in Table 1. SPF values for both ZnO films (35 and 37) correspond to the protection category "good" [7] or "very good" [1]. Similarly to [1], the best protection against UV radiation was obtained with nanostructured thin ZnO:In film, whose SPF equals 116, so, its 50+ protection category is "excellent".

Fig. 5a, b, c show SEM images of three thin nanostructured CuI films deposited on the PET tapes by the SILAR technique using different concentrations of the anionic precursor NaI, as indicated in Table 2. It is seen that all CuI films are homogeneous, but rougher compared to the uncoated PET tape in Fig. 5d. Especially loose are CuI films obtained in the more dilute anionic precursor, namely 0.59 μm thick CuI film deposited using 0.075 M NaI (Fig. 5b) and 0.1 μm thick CuI film deposited using 0.05 M NaI (Fig. 5c).

Chemical XRF microanalysis has revealed (Fig. 6, Table 2) that all CuI films are enriched with copper regardless of the SILAR mode (Cu/I atomic ratio is ~ 1.3-1.4). Some other elements are observed in the XRF spectra. Among them, C and O mainly belong to the PET tape. Small peaks of Al are observed in the XRF spectra (EDS of Al is not present in Table 2) apparently generated by aluminum table and holder for the samples of the vacuum chamber, in which XRF microanalysis was carried out. In addition, all CuI films obtained via SILAR contain sulfur from the chemically unstable compound sodium thiosulfate $Na_2S_2O_3$ in the cationic precursor solution. According to [19], sulfur as an element of the sixth group is able to form acceptor levels in the copper iodide without the formation of copper sulphide phases distinguishable via XRD analysis.

Fig. 7 demonstrates experimental XRD patterns for these copper iodide films deposited on PET tapes (a, b, and c) and also XRD pattern of the uncoated PET tape (d). As seen in Fig. 7, each XRD pattern of CuI film on PET substrate contains some diffraction peaks, which belong to cubic Marshite copper iodide structure (zinc blende, γ-CuI, JCPDS # 06-0246). So, all CuI films are single-phase and polycrystalline. Calculations of the average crystallite size D yielded 31 nm values for thicker CuI films (with $t = 0.59$ μm and $t = 0.82$ μm) made using more concentrated anionic precursors (0.075 M and 0.1 M NaI, respectively). The value $D = 18$ nm was obtained for the thinnest CuI film (with $t = 0.10$ μm) deposited from the diluted anionic precursor 0.05 M NaI (Table 2).
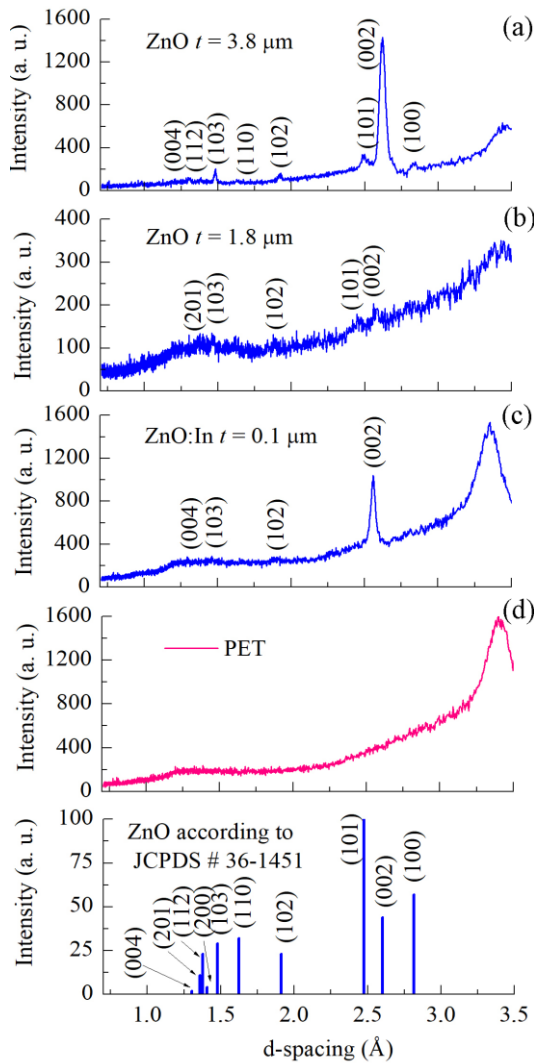
Fig. 3 – XRD patterns of ZnO (a, b) and ZnO:In (c) films with thickness *t*, which were deposited via different SILAR modes on PET, and XRD pattern of the uncoated PET tape (d)
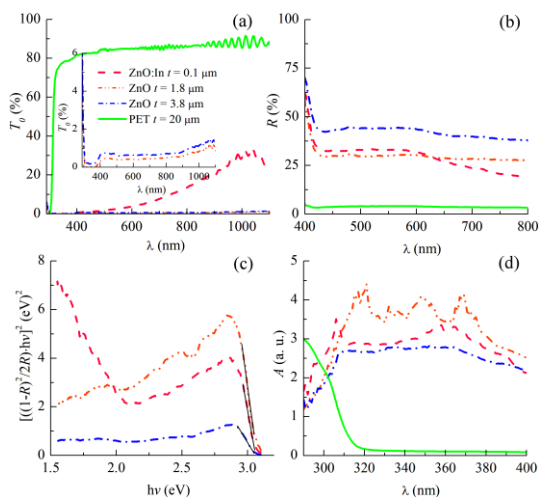

Fig. 4 – Optical properties of ZnO and ZnO:In films with thickness *t*, which were deposited via different SILAR modes on PET tapes, and optical properties of the uncoated PET tape: (a) − optical transmission spectra $T_o(\lambda)$; (b) − diffuse re-flectance spectra $R(\lambda)$; (c) – graphs for E_g found by means of the Kubelka-Munk function $F(R)$; (d) − UV-absorption spectra $A(\lambda)$
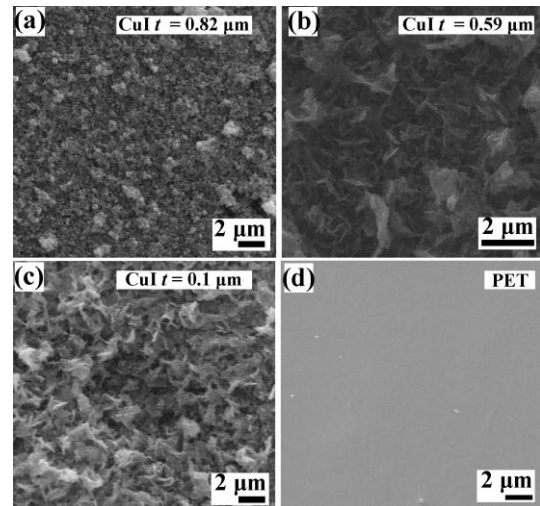

Fig. 5 – SEM images of CuI films (a, b, c) with thickness *t* deposited via SILAR on PET tapes using different concentrations of the anionic precursor NaI: (a) 0.1 M; (b) 0.075 M; (c) 0.05 M; (d) SEM image of the uncoated PET tape

Fig. 6 – SEM images of CuI films (a, b, c) with thickness *t* deposited via SILAR on PET tapes using different concentrations of the anionic precursor NaI: (a) 0.1 M; (b) 0.075 M; (c) 0.05 M; (d) SEM image of the uncoated PET tape
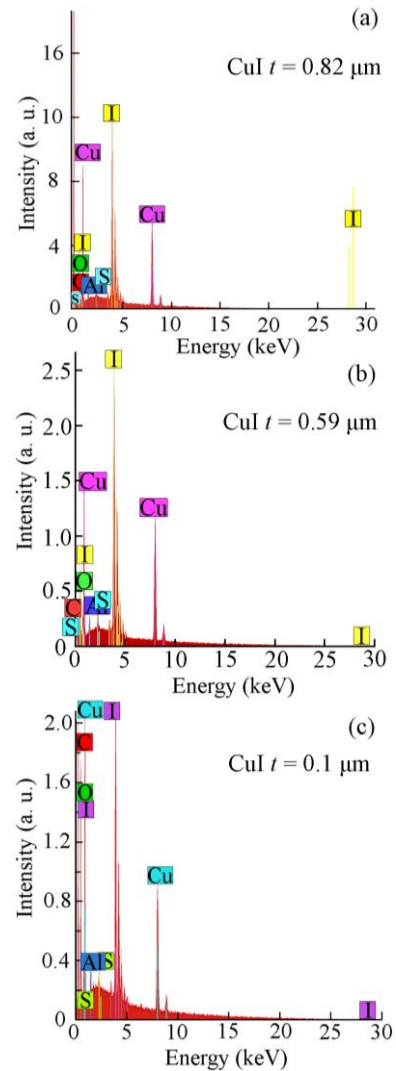
Table 2 – SILAR modes for CuI films on PET substrates; thickness, chemical composition, crystal structure, and UV-shielding ability of these films

Material	Anionic precursor NaI, M	Film thickness, µm	Chemical composition according to EDS, at. %					Crystal structure according to XRD			UV-protection factor SPF (290-400 nm)
			Cu	O	I	S	C	D, nm	$\varepsilon \cdot 10^3$, a.u.	$1/D^2 \cdot 10^{-15}$, lines·m^{-2}	
CuI	0.1	0.82	26	17	19	1	36	31	4	1.0	25
CuI	0.075	0.59	26	18	20	2	32	31	3	1.0	32
CuI	0.05	0.10	6	30	4	< 1	59	18	6	3.1	21
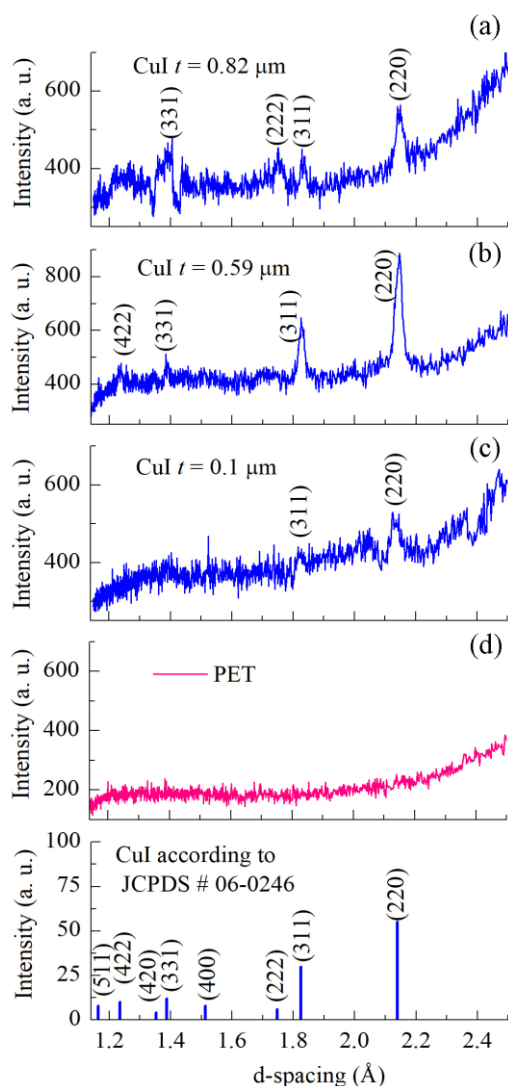
Fig. 7 – XRD patterns of CuI films (a, b, c) with thickness t deposited via SILAR on PET tapes using different concentrations of the anionic precursor NaI: (a) 0.1 M; (b) 0.075 M; (c) 0.05 M; (d) SEM image of the uncoated PET tape

Analysis of structural parameters of copper iodide films has revealed small tensile lattice microstrains $\varepsilon = (3-6) \cdot 10^{-3}$ a.u. and low dislocation densities $1/D^2 = (1.0-3.1) \cdot 10^{15}$ lines/m^2, approximately the same as in ZnO and ZnO:In films deposited by us using the SILAR method (compare Table 1 and Table 2).

Fig. 8 shows optical properties of CuI films deposited via SILAR on PET substrates. All CuI films are semi-transparent in the visible range, their maximum transparency T_0 decreases with an increase of the film thickness from 7 to 2.5 % (Fig. 8a). Due to the large surface roughness of CuI films (see Fig. 5a, b, c) their optical reflections are predominantly diffuse. The $R(\lambda)$ spectra in Fig. 8b confirm the significant reflectance in the entire visible range. The band gaps E_g for direct optical transitions in deposited via SILAR CuI films obtained from the Kubelka-Munk function (Fig. 8c) are in the range of 2.9-3.0 eV (Table 2).

It is close to the value of 2.95-3.1 eV for bulk CuI at near-room temperature [10, 12]. From the comparison of the absorption spectra in Fig. 4d and Fig. 8d, it is seen that all CuI films quite strongly absorb light in the UV range similarly to the undoped zinc oxide films deposited via SILAR. However, UV-protection ability of these CuI films in the shorter wavelength UV part (from the solar UVB in the 290-308 nm range) is worse than for ZnO:In films prepared via SILAR.
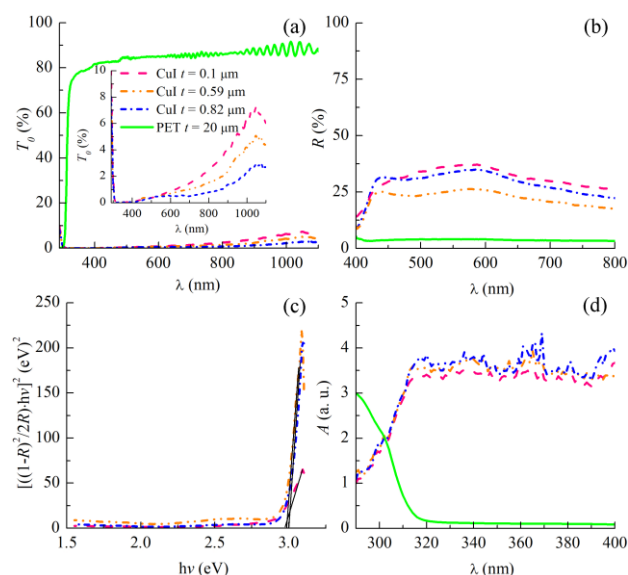
Fig. 8 – Optical properties of CuI films with thickness t which were deposited by SILAR on PET tapes using various concentrations of anionic precursor NaI, according to Table 2, and optical properties of the uncoated PET tape: (a) optical transmission spectra $T_0(\lambda)$; (b) diffuse reflectance spectra $R(\lambda)$; (c) graphs for the E_g finding by means of the Kubelka-Munk function $F(R)$; (d) UV-absorption spectra $A(\lambda)$

Sun protection factors calculated in accordance with an international standard ISO 2443:2012 (E) for CuI films deposited via SILAR on PET substrates are presented in Table 2. The SPF values for CuI films are from 21 to 32 that correspond to the protection category "good" [1, 7].

Table 3 – UV-protection ability of the samples consisting of the PET substrate and the nanocrystalline film deposited on it by the SILAR method

Sample consisting of the films with the thickness t	UV-protection factor SPF (290-400 nm)
CuI ($t = 0.10$ µm)/PET ($t = 20$ µm)	62
CuI ($t = 0.59$ µm)/PET ($t = 20$ µm)	73
CuI ($t = 0.82$ µm)/PET ($t = 20$ µm)	66
ZnO ($t = 3.8$ µm)/PET ($t = 20$ µm)	76
ZnO ($t = 1.8$ µm)/PET ($t = 20$ µm)	78
ZnO:In ($t = 0.10$ µm)/PET ($t = 20$ µm)	157

It should be noted that the sun protection factor values given in Table 1 and Table 2 for ZnO, ZnO:In and CuI films, respectively, were obtained on the basis of the optical transmission spectra measured relative to the PET substrate, that is, they do not include UV absorption by the PET substrate itself. At the same time, the significant absorption of UVB by the PET tape is clearly seen in Fig. 4d and Fig. 8d. Calculations according to standard ISO 2443:2012 (E) showed that the UPF rating of the PET tape equals to 41, since it is UVB that is dangerous in terms of the health care. By summing up the sun protection factors for the PET tape and for the films deposited on PET via SILAR, we obtained data on the UV-protection ability of the film samples presented in Table 3. It is seen that all the samples have SPF 50+, i.e. their protection category is "excellent".

4. CONCLUSIONS

In this study, thin nanostructured films of pure and indium-doped zinc oxide made by the cheap, affordable and suitable for mass production SILAR method, as well as thin nanostructured films of copper iodide obtained by the same method on thin flexible cheap poly(ethylene terephthalate) tapes have been proposed as a new material for UV-shielding applications. UV-protection ability of the film samples consisting of the PET substrate and the film deposited on it by the SILAR method fits in accordance with an international standard ISO 2443:2012(E) "Determination of sunscreen UVA photoprotection in vitro" the category "excellent" (50+). The best low cost flexible and lightweight UV-shielding material turned out to be that consisted from ZnO:In film and PET substrate.

The authors declare no competing interest.

REFERENCES

1. M. Sasani Ghamsari, S. Alamdari, W. Han, H.-H. Park, *Int. J. Nanomed.* **12**, 207 (2016).
2. T. Li, B. Li, Y. Ji, L. Wang, *Polymers* **10**, 1112 (2018).
3. J. Li, C. Yao, S. Zuo, W. Liu, Z. Li, S. Luo, A. Xie, *Nano Adv.* **2**, 8 (2017).
4. U.G.M. Ekanayake, N. Rathuwadu, M.M.M.G.P.G. Mantilaka, R.M.G. Rajapakse, *RSC Adv.* 8, 31406 (2018).
5. S. Anitha, T.S. Natarajan, *J. Nanosci. Nanotechnol.* **15**, 9705 (2015).
6. Y. Tu, L. Zhou, Y.Z. Jin, C. Gao, Z.Z. Ye, Y.F. Yang, Q.L. Wang, *J. Mater. Chem.* **20**, 1594 (2010).
7. A. Verbič, M. Gorjanc, B. Simončič, *Coatings* 9, 550 (2019).
8. V. Pandiyarasan, S. Suhasini, J. Archana, M. Navaneethan, A. Majumdar, Y. Hayakawa, H. Ikeda, *Appl. Surf. Sci.* **418**, 352 (2017).
9. R. Li, J. Che, H. Zhang, J. He, A. Bahi, F. Ko, *J. Nanopart. Res.* **16**, 2581 (2014).
10. M. Grundmann, F.-L. Schein, M. Lorenz, T. Böntgen, J. Lenzner, H. von Wenckstern, *phys. status solidi a* **210**, 1671 (2013).
11. B.N. Ezealigo, A.C. Nwanya, A. Simo, R.U. Osuji, R. Bucher, M. Maaza, F.I. Ezema, *Arabian J. Chem.* (2017).
12. G. Apsana, P.P. George, N. Devanna, R. Yuvasravana, *J. Bionanosci.* **12**, 191 (2018).
13. A. Pramanik, D. Laha, D. Bhattacharya, P. Pramanik, P. Karmakar, *Colloid. Surf. B* **96**, 50 (2012).
14. N.P. Klochko, K.S. Klepikova, S.I. Petrushenko, S.V. Dukarov, V.R. Kopach, I.V. Khrypunova, D.O. Zhadan, V.M. Lyubov, A.L. Khrypunova, *Radiat. Phys. Chem.* **164**, 108380 (2019).
15. N.P. Klochko, K.S. Klepikova, V.R. Kopach, D.O. Zhadan, V.V. Starikov, D.S. Sofronov, I.V. Khrypunova, S.I. Petrushenko, S.V. Dukarov, V.M. Lyubov, M.V. Kirichenko, S.P. Bigas, A.L. Khrypunova, *J. Mater. Sci. – Mater. Electron.* **30**, 17514 (2019).
16. N.P. Klochko, K.S. Klepikova, S.I. Petrushenko, V.R. Kopach, G.S. Khrypunov, D.O. Zhadan, S.V. Dukarov, V.M. Lyubov, M.V. Kirichenko, S.V. Surovitskiy, A.L. Khrypunova, *J. Nano-Electron. Phys.* **10** No 6, 06038 (2018).
17. N.P. Klochko, V.R. Kopach, I.I. Tyukhov, G.S. Khrypunov, V.E. Korsun, V.O. Nikitin, V.M. Lyubov, M.V. Kirichenko, O.N. Otchenashko, D.O. Zhadan, M.O. Maslak, A.L. Khrypunova, *Sol. Energy.* **157**, 657 (2017).
18. S.K. Kuanr, G. Vinothkumar, K.S. Babu, *Mater. Sci. Semicond. Process.* **75**, 26 (2018).
19. N.P. Klochko, K.S. Klepikova, V.R. Kopach, I.I. Tyukhov, D.O. Zhadan, G.S. Khrypunov, S.I. Petrushenko, S.V. Dukarov, V.M. Lyubov, M.V. Kirichenko, A.L. Khrypunova, *Sol. Energy.* **171**, 704 (2018).

Наноструктуровані тонкі плівки ZnO і CuI на полі(етілентерафталатних) стрічках для захисту від ультрафіолетового випромінювання

Н.П. Клочко[1], К.С. Клепікова[1], Д.О. Жадан[1], В.Р. Копач[1], І.В. Хрипунова[1], С.І. Петрушенко[2], С.В. Дукаров[2], В.М. Любов[1], А.Л. Хрипунова[1]

[1] *Національний технічний університет «Харківський політехнічний інститут», вул. Кирпичова 2, 61002 Харків, Україна*
[2] *Харківський національний університет імені В.Н. Каразіна, площа Свободи 4, 61022 Харків, Україна*

У роботі ми вивчаємо придатність для захисту від земної ультрафіолетової частини сонячного спектра нелегованих і легованих індієм тонких наноструктурованих плівок оксиду цинку, ZnO і ZnO:In, відповідно, і плівок йодиду міді (CuI), отриманих методом послідовної адсорбції та реакції іонних шарів (SILAR) на легких і недорогих гнучких підкладках з полі(етілентерефталата) (ПЕТ). Морфологія плівки спостерігалася методом скануючої електронної мікроскопії (SEM). Хімічний склад плівок досліджено методом рентгенофлуоресцентного (XRF) мікроаналізу. Для дослідження кристалічної структури ми використовували рентгенодифракційний метод (XRD). Здатність УФ захисту наноструктурованих тонких плівок, стрічок ПЕТ і зразків, що складаються з підкладок ПЕТ і плівок, нанесених на них методом SILAR, була оцінена на основі їх оптичних властивостей відповідно до міжнародного стандарту ISO 2443:2012 (E) «Визначення фотозахисту від УФА сонцезахисних кремів in vitro». Згідно з дослідженням, наноструктуровані тонкі плівки ZnO, ZnO:In і CuI, виготовлені дешевим, доступним і придатним для масового виробництва методом SILAR на тонких гнучких дешевих ПЕТ підкладках, були запропоновані в якості нового матеріалу для застосування в області екранування від ультрафіолетового випромінювання. Відповідно до міжнародного стандарту ISO 2443:2012 (E) здатність до УФ-захисту зразків, що складаються з ПЕТ-підкладок і плівок, нанесених на них методом SILAR, відповідає категорії «відмінно» (50+). Кращим недорогим, гнучким і легким матеріалом, що захищає від ультрафіолетового випромінювання, виявився матеріал, що складається з плівки ZnO:In і ПЕТ підкладки, у якого сонцезахисний коефіцієнт дорівнює 157.

Ключові слова: ZnO, CuI, Полі(этілентерефталат), Ультрафіолетове випромінювання, Сонцезахисний коефіцієнт.